



## An Egyptian Sandstone Deposit as a Source of Good Quality Kaolin and Ultra-Pure Silica Sand: Sample Characterization and Separation (Part I)

By Suzan S. Ibrahim, Wael M. Fathy, Magdy A. Elsayed, Abd El-hady M. Saleh,  
Tawfik R. Boulos & Mohamed R. Moharam

*Al-Azhar University*

**Abstract-** A kaolinitic sandstone sample from Wadi Qena deposit, the Eastern Desert of Egypt, was subjected to mineralogical and chemical characterization for possible separation of kaolin and silica sand concentrates. Attrition scrubbing process was applied in two different scenarios either on the whole crude sample or on the separate size fractions to collect both the white kaolin coating the sand grains and the sand itself. Factors affecting the process and the products after attrition were optimized and evaluated.

The -0.025 mm kaolin product after the attrition scrubbing process assays 36.05% Al<sub>2</sub>O<sub>3</sub>, 47.72% SiO<sub>2</sub>, 0.62% Fe<sub>2</sub>O<sub>3</sub> and 1.67% TiO<sub>2</sub>. The X-ray diffraction analysis of the kaolin product shows sharp, narrow kaolin peaks and reflects the high degree of ordering. Its brightness and whiteness optical measures satisfy the requirements of the local paper industry.

**Keywords:** cellular kaolinitic sandstone, classification, attrition scrubbing, fine kaolin, silica sand.

**GJRE-G Classification:** FOR Code: 290502



*Strictly as per the compliance and regulations of:*



# An Egyptian Sandstone Deposit as a Source of Good Quality Kaolin and Ultra-Pure Silica Sand: Sample Characterization and Separation (Part I)

Suzan S. Ibrahim<sup>α</sup>, Wael M. Fathy<sup>σ</sup>, Magdy A. Elsayed<sup>ρ</sup>, Abd El-hady M. Saleh<sup>ω</sup>, Tawfik R. Boulos<sup>ξ</sup>  
& Mohamed R. Moharam<sup>§</sup>

**Abstract-** A kaolinitic sandstone sample from Wadi Qena deposit, the Eastern Desert of Egypt, was subjected to mineralogical and chemical characterization for possible separation of kaolin and silica sand concentrates. Attrition scrubbing process was applied in two different scenarios either on the whole crude sample or on the separate size fractions to collect both the white kaolin coating the sand grains and the sand itself. Factors affecting the process and the products after attrition were optimized and evaluated.

The -0.025 mm kaolin product after the attrition scrubbing process assays 36.05% Al<sub>2</sub>O<sub>3</sub>, 47.72% SiO<sub>2</sub>, 0.62% Fe<sub>2</sub>O<sub>3</sub> and 1.67% TiO<sub>2</sub>. The X-ray diffraction analysis of the kaolin product shows sharp, narrow kaolin peaks and reflects the high degree of ordering. Its brightness and whiteness optical measures satisfy the requirements of the local paper industry.

On the other hand, the attritioned white sand product assays 0.036% Fe<sub>2</sub>O<sub>3</sub> and 0.119% Al<sub>2</sub>O<sub>3</sub>. This sand product matches the specifications for tableware and colorless glass containers industries.

**Keywords:** kaolinitic sandstone, classification, attrition scrubbing, fine kaolin, silica sand.

## I. INTRODUCTION

In Egypt, distributions of kaolinitic sandstones rocks are present in Sinai, the Eastern Desert, and the southern Western Desert, Figure 1, [1-4]. Wadi Qena is one of the largest wadies in the Eastern Desert of Egypt. It is constituted from sandstones which are represented by quartz arenite, while kaolinite is the sole clay mineral constituent. These sandstones are being inherited from felsic- granitic and reworked quartzose sediments and transported by rivers to the basin of deposition, [5-14].

Kaolinite and silica sands are belonging to the group of industrial minerals, where their characteristic features lie in their physical properties (e.g., fibrosity of asbestos, insulatory properties of mica, the high specific gravity of barite). However, kaolinite has the chemical composition Al<sub>2</sub>O<sub>3</sub>•2SiO<sub>2</sub>•2H<sub>2</sub>O. It is produced by the

chemical weathering of aluminum silicate minerals like feldspar. The main use of the mineral kaolinite (about 50%) is paper production; its use ensures the gloss on some grades of coated paper. Kaolin is also used in ceramics, in toothpaste, and in paint to extend the titanium dioxide (TiO<sub>2</sub>) white pigment and modify gloss levels. In its altered metakaolin form, it is used as a pozzolan; when added to a concrete mix, metakaolin accelerates the hydration of Portland cement, [15-17].

On the other hand, silica sands have got the most diversified use among all the non-metallic minerals deposits. The white silica sands are defined as high purity sands in which the sand grains are composed entirely of quartz. Impurities are very minor including for example: iron oxides, feldspars, micas, heavy minerals (zircon, tourmaline), [15-17]. Silica is a basic material in the glass industry, ceramic and refractory industries, and silicon-based chemicals. Silica sand is evaluated for industrial use on the basis of its chemical composition and physical properties. However, chemical specification is of paramount importance in glassmaking, whereas grain angularity and hardness are important for sandblasting, [15-17].

The present study is devoted towards the full mineralogical and chemical characterization of Wadi Qena sandstone rock for possible separation of its main constituents: kaolin and silica sand components. Further treatment of these mineral components to satisfy the requirements of the industry is the appropriate objective.

## II. EXPERIMENTAL, MATERIAL AND TECHNIQUES

A kaolinitic sandstone sample was supplied through the Egyptian Geological Survey and Mining Authority from Wadi-Qena deposit; northern Eastern Desert of Egypt. A representative sample of which was prepared and subjected to mineralogical and chemical evaluation. The petrographic examination microscope examination of the grain composition and texture are applied using an Olympus optical microscope. Powders were prepared from the same sample and were subjected to phase and chemical analysis using a Philips PW 1730 X-ray generator with Fe-filtered Co K $\alpha$  radiation, run at 40 kV and 30 mA and A Philips PW

**Author  $\alpha$   $\xi$ :** Central Metallurgical Research and Development Institute (CMRDI), P.O. Box 87 Helwan, 11421 Cairo, Egypt.

e-mails: [suzansibrahim@gmail.com](mailto:suzansibrahim@gmail.com), [TRBoulos@gmail.com](mailto:TRBoulos@gmail.com)

**Author  $\sigma$   $\rho$   $\omega$   $\xi$ :** Al-Azhar University, Faculty of Engineering, Mining and Petroleum Dept., Cairo, Egypt. e-mails: [wael\\_fathy@egyptire.com](mailto:wael_fathy@egyptire.com), [magdyabdo970@yahoo.com](mailto:magdyabdo970@yahoo.com), [amsaleh2006@yahoo.com](mailto:amsaleh2006@yahoo.com), [moreda\\_45@yahoo.com](mailto:moreda_45@yahoo.com)

2400 X-ray spectrometer with a tube voltage and current for a W target of 40 kV and 60 mA, respectively. The dry/wet particle size analyses were conducted using a standard series of Tyler sieves and a Lazer particle size

analyzer model (COR 2001). The optical properties of different kaolin products were measured using TMI Brightness & Color Meter JY9800, Model No. 68-59-00-002.

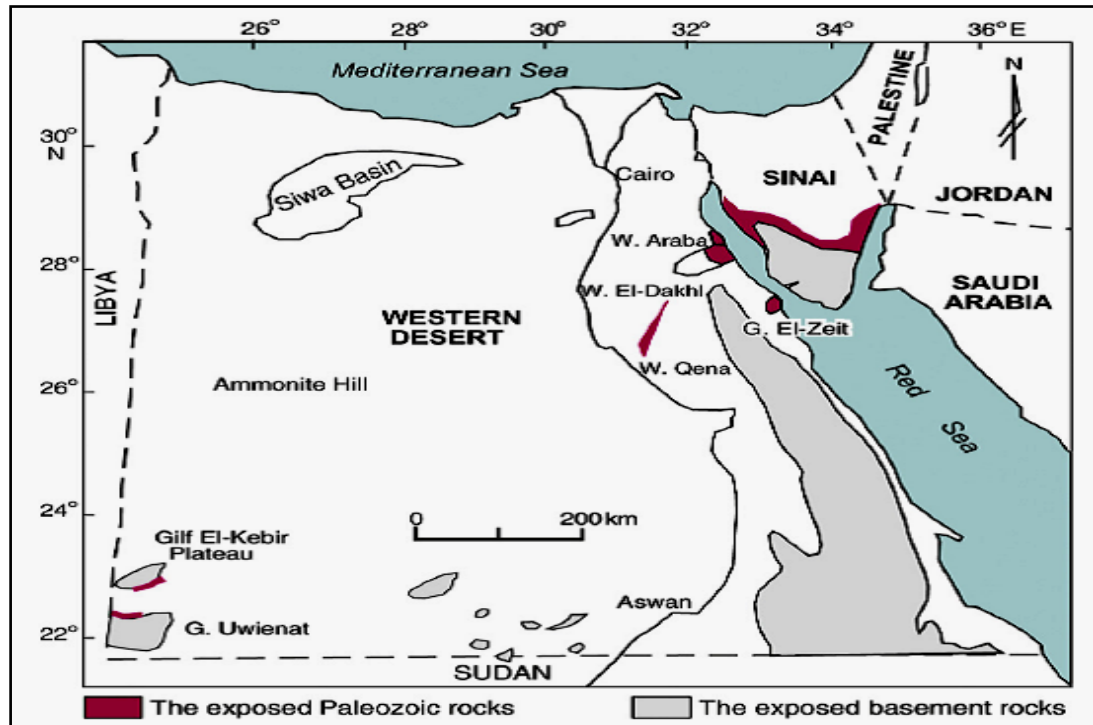


Figure 1: Location map showing the areas of the main kaolinitic sandstones distributions in Egypt, [13]

The attrition scrubbing tests were conducted using a 5 liter Pyrex glass container of a Denver 12 flotation cell. Two attrition scrubbing scenarios according to the type of feeding material were applied. The indicator of prevailing was the amount of the produced kaolin product (the 25-micron product) and its grade concerning the optical properties, mainly the whiteness and the brightness were determined. The first scenario was the attrition scrubbing of the overall sandstone sample as received. The second scenario was to gather the 25-micron products after the separate attrition scrubbing of the dry classified the +0.60 mm fraction, the -0.6+0.10 mm fraction, and the -0.10 mm fraction. The attrition time optimized in this study. Other vital parameters like pulp solid% and the attrition impeller speed were kept constant at the maximum predetermined levels (65% solid and 2700 rpm) throughout all the experiments. The silica sand and kaolin products after the optimized attrition scrubbing process were evaluated for the local industry.

### III. RESULTS AND DISCUSSION

#### a) Characterization of the Head Sample

The x-ray diffraction analysis of the head sample shows the presence of silica and kaolin

minerals, Figure 2. It contains 89.97% silicon dioxide, 6.95% alumina, 0.138% iron oxide, and 0.356% titanium oxide, Table 1. SEM photomicrograph shows that the original sample is composed of large to medium quartz grains cemented with white kaolin which appeared mainly as grain rimming and coatings of the silica quartz grains, Figure 3. SEM photomicrograph shows also quartz grains with conchoidal fractures, straight grooves, and crescent gouges, which suggests its deposition in moderate to high energy aqueous environments, [18-21]. The surface textures of the quartz grains indicate that they are the product of mechanical weathering, [18-21].

The microscopic investigation of the sample shows heavy minerals inclusions on the sand surfaces, Figure 4. After the sink/float separation (using bromo form), it is noticed that black and colored particles are more enriched in the fine fractions below 100 micron. These minerals are mainly rounded grains of zircon, tourmaline, and rutile, Figure 4. This suggests that the deposit derivation was either from igneous or metamorphic rocks, [18-21]. The presence of needle and round crystals of biotite and of fine magnetite grains was confirmed.

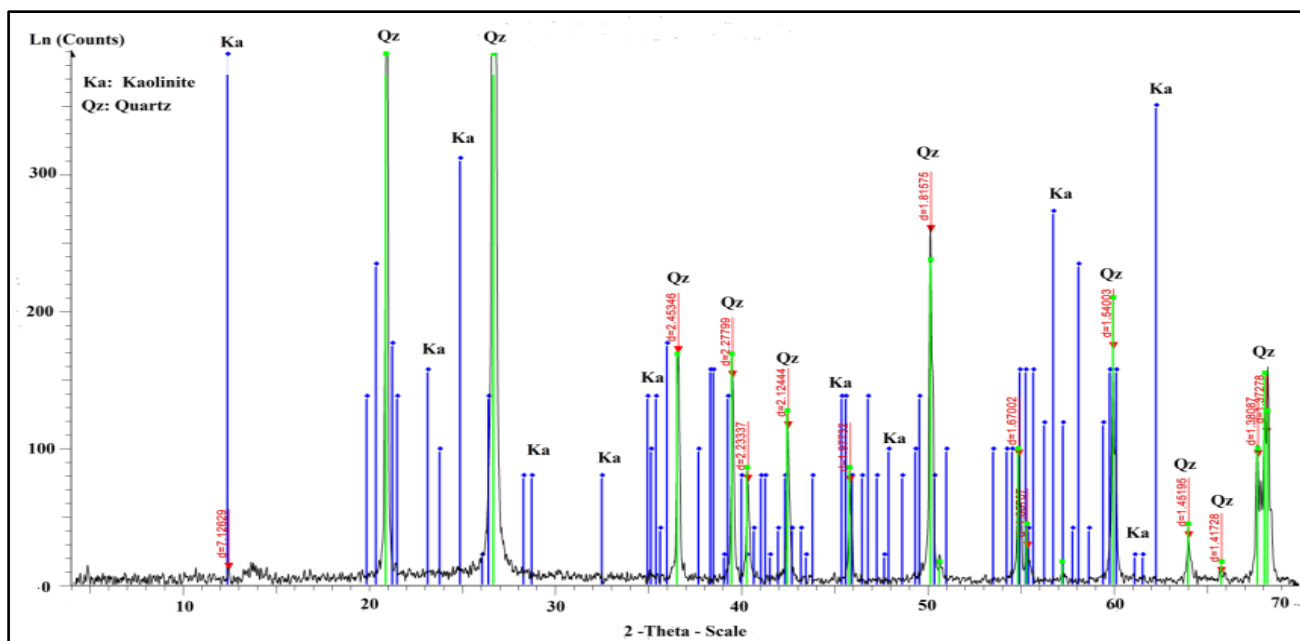


Figure 2: The X-ray diffraction analysis of the rock head sample

Table 1: Complete chemical analysis of the head sample

Constituent	Wt.%
SiO <sub>2</sub>	89.968
Al <sub>2</sub> O <sub>3</sub>	6.952
Fe <sub>2</sub> O <sub>3</sub>	0.138
TiO <sub>2</sub>	0.356
SrO	0.021
CaO	0.192
Na <sub>2</sub> O	0.065
K <sub>2</sub> O	0.022
P <sub>2</sub> O <sub>5</sub>	0.061
Cl	0.072
SO <sub>3</sub>	0.213
ZrO <sub>2</sub>	0.040
L.O.I	1.90

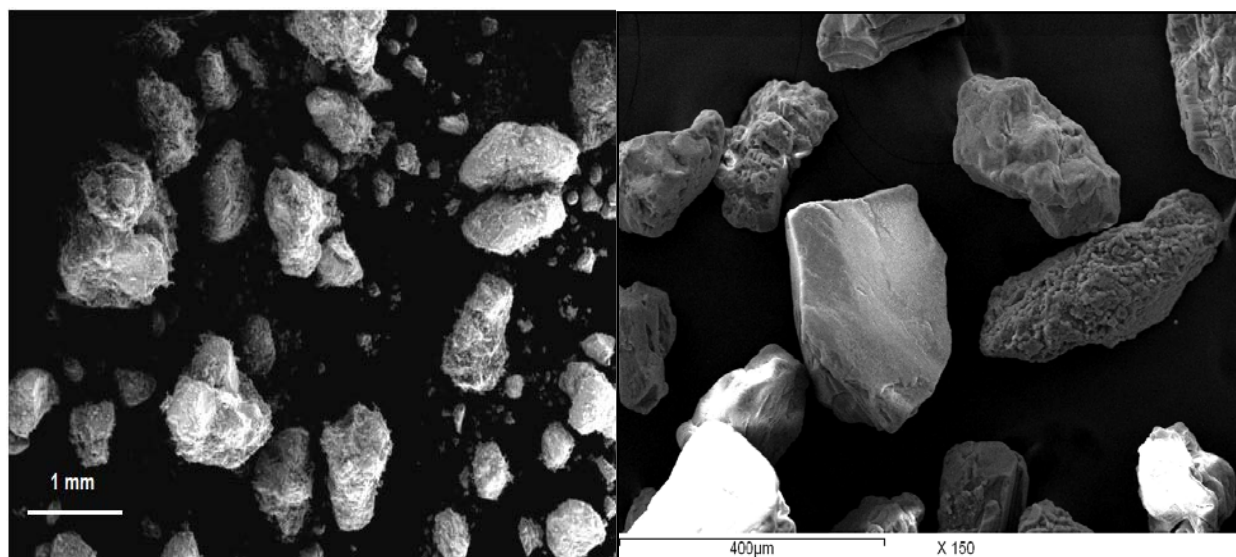


Figure 3: SEM photomicrograph of the head sample

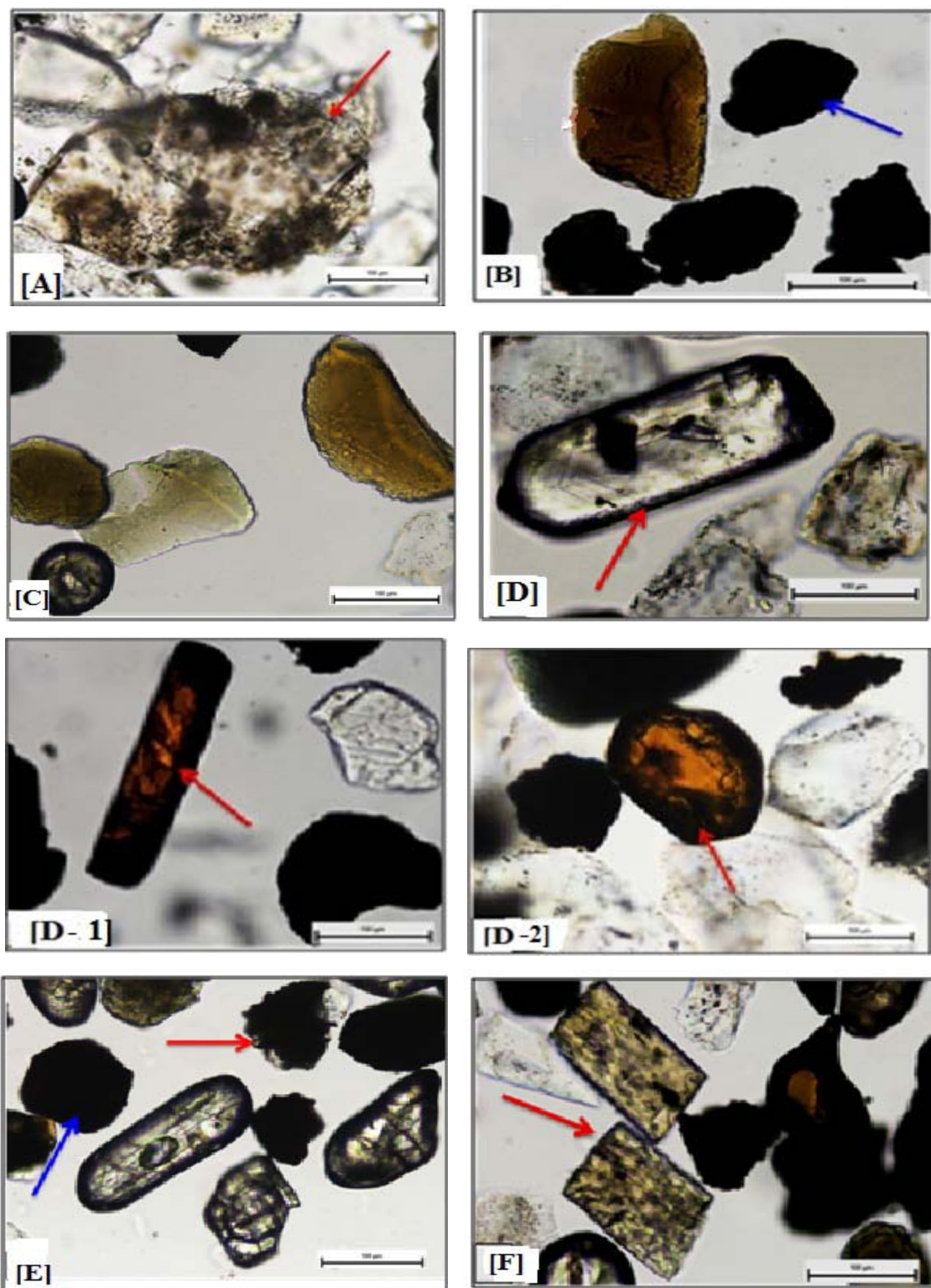


Figure 4: Photomicrograph of different gangue minerals found in the head sample

[A]: Inclusions in silica grains, [B]: iron oxides, [C]: Biotite, [D, D-1, and D-2]: different forms of Rutile, [E]: Zircon, and [F]: Tourmaline

b) *The Dry/ Wet Classification of the Head Sample*

The chemical analysis of the dry and wet classified products shows great upgrading in the sand quality compared to the original head sample, Tables 2 and 3. The silica content increases from 89.97% in the feed sample to 96.97% in the dry classified -0.60+0.106 mm sand product. Additionally, the dry classification of the head sample helped to reduce the iron oxide content from 0.138% in the feed sample to 0.065% in the dry classified product, Table 3, with removal yield reaching 53%. The sand upgrading is due to the rejection of most iron oxides minerals, mainly magnetite below 100 micron.

In addition, the alumina content decreased from 6.95% in the head sample to 2.57% in the dry classified sand product with a removal yield reaching 63%. This is due to the separation of most of the free kaolin particles to below 100 micron, and in addition to the rejection of aluminum bearing minerals that are below 100 micron like biotite. On the other hand, titanium oxide is reduced from 0.36% in the head sample to 0.128% in the dry classified sand sample due to the separation of rutile particles by screening to below 100 micron, with 64% removal yield, Table 3.

It is noticed that wet screening of the head sample has no effect on the sand grade despite the notable change in the particle size distribution of the 0.60+0.106 mm products before and after the wet screening, Table 3. This change in the particle size distribution is due to the disintegration of the sandstone accumulations in the +0.60 mm fraction which represents 11.74% by overall weight of the head sample by just simple water showering. This data illustrates how much the clusters fragility of the present sandstone sample is, while it does not need any crushing process to disintegrate into individual grains. However, this water showering is not enough to take off the kaolin coatings that cover the surfaces of the silica grains, and this may be the reason why the grade of the washed sample is not affected by the water washing process, Table 3.

Table 2: The dry and wet sieve analysis of the classified products

Size fraction, um	Dry Classification		Wet Classification	
	Wt., %	Cum. wt., retained %	Wt., %	Cum. wt., retained %
+600	11.74	11.74	1.32	1.32
- 600 + 106	79.76	91.50	87.28	88.60
-106+45	2.37	93.87	2.53	91.13
-45+ 25	0.98	94.85	1.42	92.55
-0.025	5.15	100.00	7.45	100.00
Total	100.00		100.00	

Table 3: The Chemical analysis of the dry and wet classified -0.60+0.106 mm sand products

Constituent	Wt.% (dry classified)	Wt.% (wet classified)
SiO <sub>2</sub>	96.97	97.050
Al <sub>2</sub> O <sub>3</sub>	2.568	2.530
Fe <sub>2</sub> O <sub>3</sub>	0.065	0.051
TiO <sub>2</sub>	0.128	0.128
SrO	0.008	0.008
CaO	0.070	0.075
Na <sub>2</sub> O	0.021	0.021
K <sub>2</sub> O	0.007	0.008
P <sub>2</sub> O <sub>5</sub>	0.017	0.015
Cl	0.023	0.021
SO <sub>3</sub>	0.056	0.054
ZrO <sub>2</sub>	0.036	0.036

c) *Attrition Scrubbing of the Sample*

After much attrition scrubbing exploratory tests on the present kaolinitic sandstone sample, it shows that the optimum attrition time for all tested samples is 3 minutes in two steps (two min followed by 1 min). Screening on 100 microns sieve with enough water showering of the over screen product after attrition scrubbing for 2 min shows to be enough to detach the kaolin coatings away from the sand surface. Attrition Scrubbing of the 100+ micron washed sand for another 1 min is sufficient to attain complete cleaning of the sand surface and to recover the most amount of the white kaolin that coat the surface of the sand grains, Tables 4-5. The 100- micron kaolin product is further screened on 25 microns sieve to reject most of the fine silica, also of the most heaviest and colored oxides that found in the range from 100 microns to 25 microns, Tables 4-5.

On the other hand, the cumulative weight percent of the produced -0.025 mm kaolin product after the attrition scrubbing of the fractionated sand sample is 1.65+4.79+4.39= 10.83% after the attrition scrubbing of the size fractions, +0.60 mm, -0.10 mm and 0.60+0.10 mm fractions, respectively, Table 5.

Table 4: Particle size distribution of the attrition product of the original head sample

Size fraction, um	Operational wt., %
+600	1.35
-600+106	84.25
-106+40	3.00
-40+25	1.45
-25	9.95
Total	100.00

**Table 5:** Operational and overall particle size distribution of the attrition products after different sand fractions  
A= +0.60 mm fraction, B= -0.10 mm fraction, C= -0.60+0.10 mm fraction

Size fraction, mm	Wt., %					
	[A]		[B]		[C]	
	Opt.	overall	Opt.	overall	Opt.	overall
+0.60	4.11	0.48	---	---	---	---
-0.60+0.106	72.11	8.47	---	---	92.83	74.02
-0.106+0.045	5.53	0.65	32.22	2.37	1.22	0.97
-0.045+0.025	4.22	0.50	11.64	0.98	0.46	0.36
-0.025	14.03	1.65	56.14	4.79	5.49	4.39
Total	100.0	11.74	100.0	8.50	100.0	79.74

i. *Evaluation of the kaolin product*

The optical properties of these kaolin fractions after the attrition scrubbing of the fractionated sand sample show lower values compared to that of the kaolin product after the attrition scrubbing of the overall sample without fractionation, Table 6. However, the kaolin product obtained after the attrition scrubbing of the 0.60+ mm fraction shows excellent optical properties measures, but it is of a relatively low weight percent compared to the head sample, Tables 5 and 6.

However, the weight percent of the produced 25- micron kaolin product after the attrition scrubbing of the head sample reaches 9.95% by overall weight, with optical properties measures reaching 79.30% brightness 85.97% iso-brightness, 92.72% whiteness, and 4.98 yellowness, Table 7.

Particle size distribution of kaolin shows that its D50 is 12.36 micron and the D80 is 23.51 micron, Figure 4. The XRD analysis of this kaolin product shows sharp narrow kaolin peaks reflect a high degree of ordering, Figure 5. Additionally, its chemical analysis shows that it contains 36.05% alumina, 47.72% silica, 0.62% iron oxide and 1.67% titanium oxide, Table 8. These chemical and optical properties specifications are

**Table 6:** Optical properties and particle size distribution measures of the 25- micron kaolin products after different samples

Sample	Brightness%	Iso-brightness%	Whiteness%	Redness%	Yellowness%	D <sub>52</sub> , um	D <sub>80</sub> , um	D <sub>96.7</sub> , um
A	79.45	86.40	92.95	0.25	5.08	11.11	21.12	36.73
B	75.09	83.07	91.14	0.34	5.96	12.36	26.16	45.22
C	77.00	85.00	92.20	0.36	5.86	11.11	23.51	40.81

**Table 7:** The optical properties and particle size distribution of the 25- micron kaolin product

Property	Measure, %	Property	Measure, %
Brightness	79.30	Yellowness%	4.98
Iso-brightness	85.97	D <sub>52</sub> , um	12.36
Whiteness%	92.72	D <sub>80</sub> , um	23.51
Redness%	0.25	D <sub>96.7</sub> , um	40.89

matching the needs of glass and ceramics industries. However, this kaolin product needs lowering its iron and titanium oxides contents to match advanced applications like paper, cosmetic and medical industries. This issue will be covered in a separate study.

Scanning electron microscope investigation of the 25- micron kaolin product records this kaolin as vermicular, euhedral and pseudo-hexagonal plates (booklets), Figure 6. The hexagonal kaolinite plates are found either as discrete individual platelet or associated with the stacks in varying sizes (up to 30 micron). The majority of kaolinite particles show parallel orientation and have face-to-edges fluctuation.

The SEM pictures of the attrition sand product show the presence of mineral remains inside the cracks cavities of the sand grains surfaces, Figure 7. In such cases, the use of ultrasonic cleaners in high- frequency range may provide cleaning for the sand surfaces where no other means of agitation is effective. The energy imparted by ultrasonic is aggressive and specific for such cases, [22].

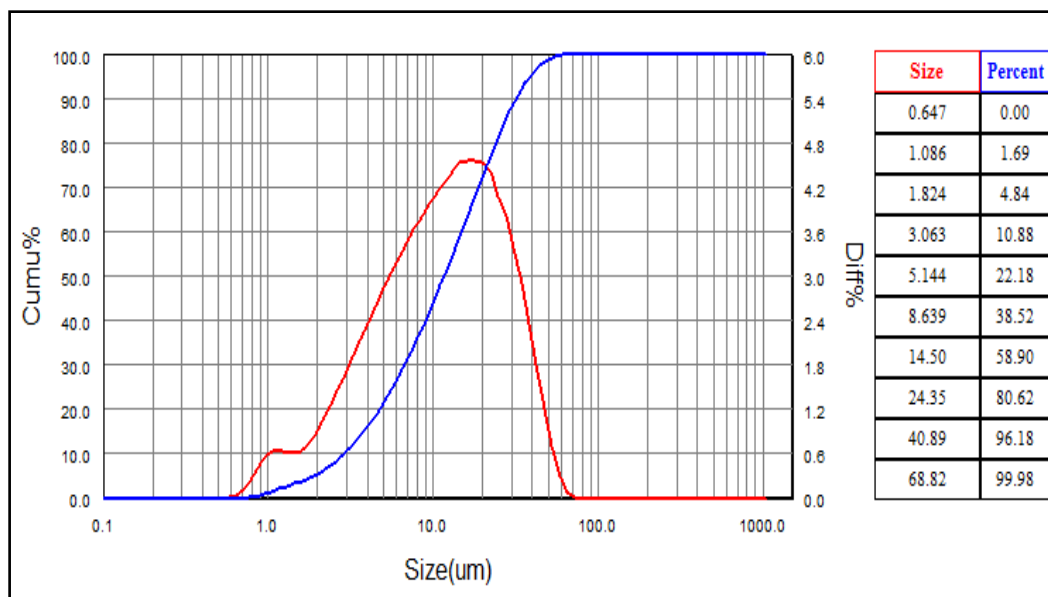


Figure 4: Particle size distribution of the kaolin product

Table 8: Chemical Analysis of the 25- micron kaolin

Constituent	Wt.%	Constituent	Wt.%
SiO <sub>2</sub>	47.72	K <sub>2</sub> O	0.04
Al <sub>2</sub> O <sub>3</sub>	36.05	P <sub>2</sub> O <sub>5</sub>	0.21
Fe <sub>2</sub> O <sub>3</sub>	0.62	Cl	0.04
TiO <sub>2</sub>	1.67	SO <sub>3</sub>	0.09
CaO	0.32	ZnO	0.01
MgO	0.16	ZrO <sub>2</sub>	0.05
Na <sub>2</sub> O	0.08	Cr	145 ppm
SrO	0.133	L.O.I	12.8

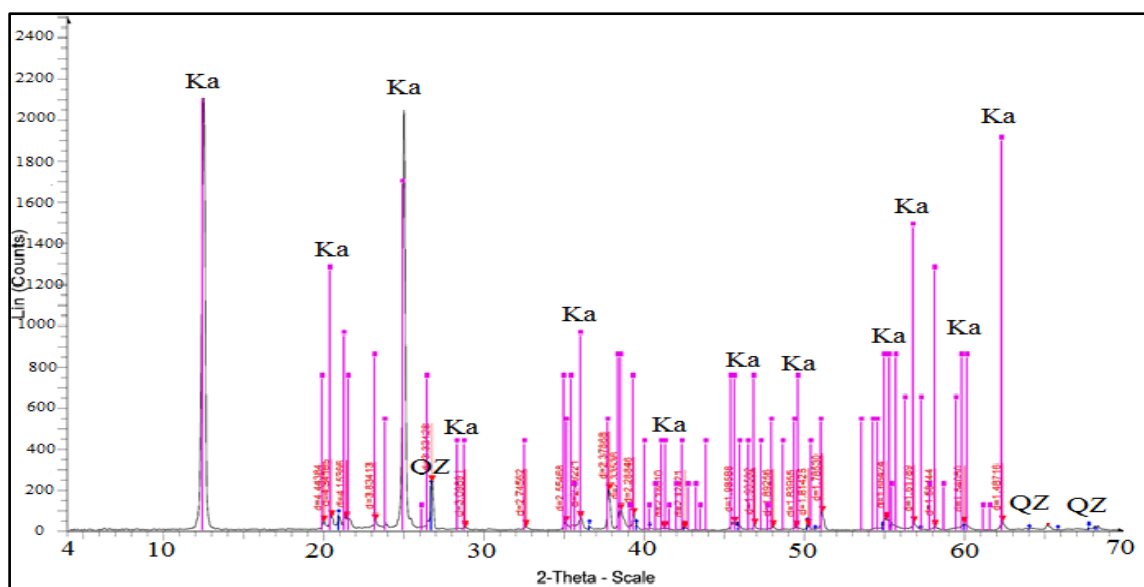


Figure 5: X-ray diffraction analysis of the kaolin product

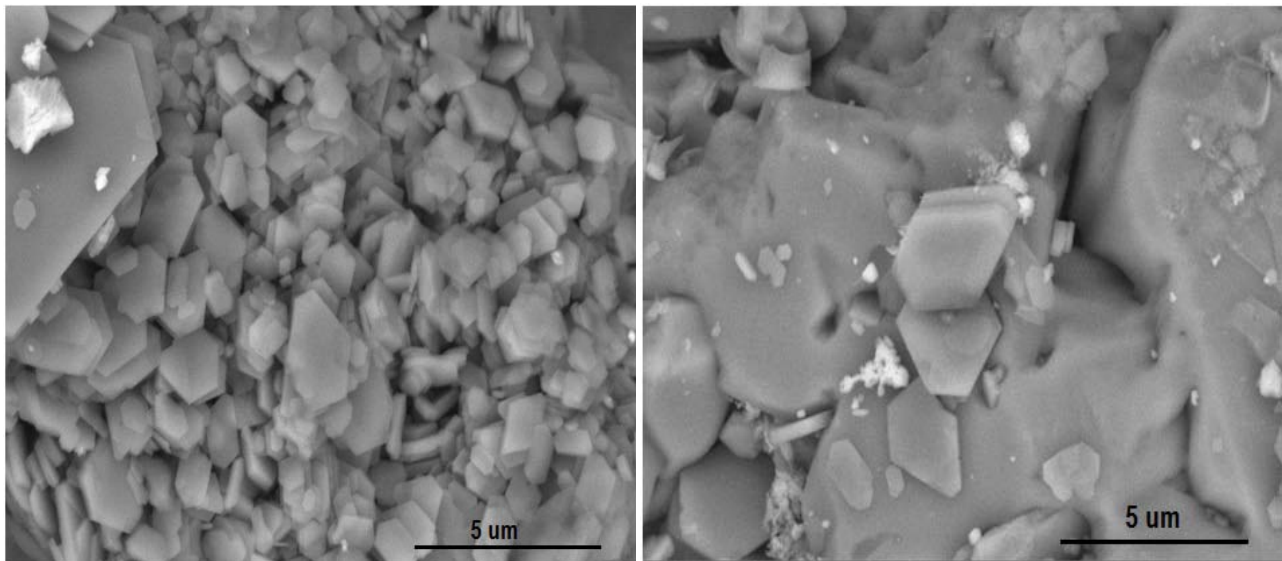


Figure 6: SEM pictures of the 25- micron kaolin product

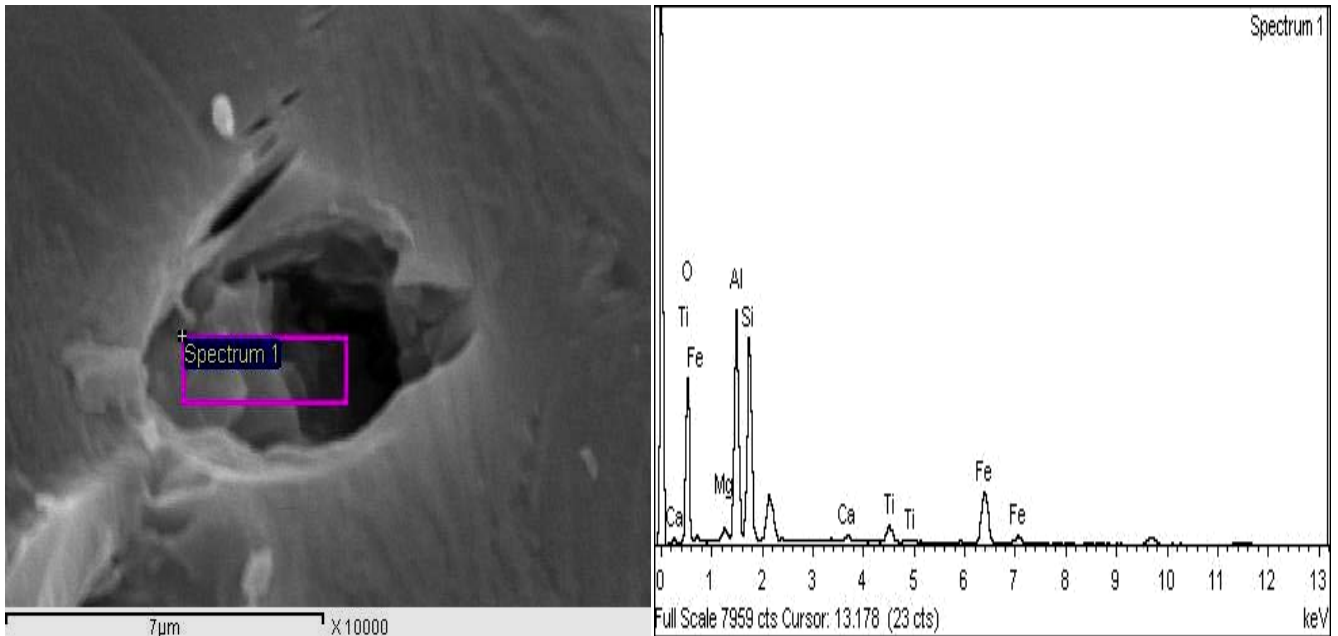


Figure 7: EDEX analysis of cavity components of an attrition sand particle

ii. Evaluation of the attrition sands

The microscopic examination of the attrition sand product shows varieties of colored and refractory minerals still present after the attrition process. These minerals include biotite, magnetite, rutile, zircon and tourmaline minerals. The iron oxide and alumina contents decrease from 0.138% and 6.952% in the feed to 0.036% and 0.119% in the attrition product, with removal yields reaching 74% and 83%, respectively, Table 9. The particle size distribution of the attrition product is depicted in Table 10. This product matches the sheet and Paper industries.

Table 9: Chemical analysis of the attrition sand product

Constituent	Wt. %
SiO <sub>2</sub>	99.754
Al <sub>2</sub> O <sub>3</sub>	0.119
Fe <sub>2</sub> O <sub>3</sub>	0.036
TiO <sub>2</sub>	0.038
CaO	0.023
P <sub>2</sub> O <sub>5</sub>	0.006
Cl	0.017
SO <sub>3</sub>	0.008
ZrO <sub>2</sub>	0.018

Table 10: Size distribution of the attrition sand product

Size fraction, mm	Wt. %	Cum. wt. % retained
-0.6	5.56	5.56
-0.420	43.18	48.74
-0.250	16.08	64.82
-0.210	22.22	87.04
-0.160	12.96	100.00
Total	100.00	

#### IV. CONCLUSION

Results show that the kaolinitic sandstone of Wadi Qena, Eastern Desert, Egypt contains notable amount of white kaolin coating the silica grains. The preferable scenario to detach this kaolin is to apply an intensive attrition scrubbing process for the whole head sample at 65% pulp solid density, 2400 rpm impeller speed for 3 min in two attrition steps separated by proper water washing step on 100 microns screen. The attrition process yields 25- micron kaolin of about 9.50% by weight of the sample. This kaolin product shows good optical properties which makes it acceptable for many domestic applications. However, it needs to minimize its iron and titanium oxides contents to match advanced applications, e.g. pharmaceutical, porcelain, and paper industries which will discuss in another issue.

On the other hand, the dry classification of the sandstone sample acts remarkable improvement in the sample grade. Further quality improving occurs after the attrition scrubbing of the whole sample. The iron and aluminum oxides decrease from 0.138% and 6.952% in the feed sample to 0.036% and 0.119% in the attrition sand product, with removal yields reaching 74% and 83%, respectively. The chemical and particle size distribution specifications of this product match the 4th grade level acceptable for plate and sheet glass industries. The attrition product needs further surface cleaning to remove the minerals remains found inside the sand surface cracks using power ultrasound treatment. Moreover, the attrition sand is in need to further processing to remove iron and heavy oxides via high intensity magnetic separation or anionic froth flotation to reach the chemical specifications of advanced types of glass applications.

#### REFERENCES RÉFÉRENCES REFERENCIAS

- Picard, L., 1942. New Cambrian fossils and Paleozoic problematic from the Dead Sea and Arabia. Bulletin of the Geology Department, Hebrew University, Jerusalem, vol. 4, issue 1, pp 1-18.
- Omara, S., 1972. An Early Cambrian outcrop in southwestern Sinai, Egypt. Neues Jahrbuch für Geologie und Paläontologie, Monatshefte 5, pp 306-314.
- Issawi, B., Hassan, M., Attia, S., 1978. Geology of Abu Tartur Plateau, Western Desert, Egypt. Annals of the Geological Survey of Egypt, 8, pp 91-127.
- Bauermann, H., 1869. Notes in geological reconnaissance made in Arabia Patraca in the spring of 1868. Geological Society of London Quarterly Journal, 25, 17-38.
- Said R., 1990. The Geology of Egypt. A. A. Balkema, Rotterdam/Brook field, 734 p.
- Said R., 1962. The Geology of Egypt. Elsevier, Amsterdam, p. 377.
- Issawi B., Jux U. 1982. Contributions to the stratigraphy of the Palaeozoic rocks in Egypt. Geological Survey, Paper 64, pp. 1-28.
- Bandel k., Kuss J., and Malchus N., 1987. The sediments of Wadi Qena, Eastern Desert, Egypt. Journal of African Earth Sciences, 6(4), pp. 427-455.
- Klitzsch E., Groschke M., and Herrmann-degen W. 1990. Palaeozoic and pre-Campanian Cretaceous strata at Wadi Qena. In: Said, R. (Ed.), "The Geology of Egypt". Rotterdam and Boston, Balkema. pp. 321-327.
- Issawi B., El-Hinnawi M. Francis M., and Mazher A. 1999. The Phanerozoic geology of Egypt, A geodynamic approach. Geol. Surv. Egypt, Spec. Publ., 76: 462 p.
- Wanas H. A. 2011. The Lower Paleozoic rock units in Egypt: An overview, China Univ. of Geosciences (Beijing), Geosciences Frontiers, 2(4). pp. 491-507.
- Abou El-Anwar, E. A., and El- Wekeil S. S. 2013. Contribution to the provenance and paleoclimate of the Lower Paleozoic sandstones of Naqus Formation, WadiQena, Northern Eastern Desert; Integration of support petrography, mineralogy and geochemistry, J. App. Sci. Res., 9 (10): pp. 6529-6546.
- Abdallah A. M., Darwish M., El-Aref M., and Helba A. A., 1992. Lithostratigraphy of the Pre-Cenomanian clastics of north Wadi Qena, Eastern Desert, Egypt, In: Sadek, A. (Ed.), Proceeding of the First International Conference on Geology of the Arab World, Cairo University, pp. 255-282.
- Abd El-Moghny, M. W. 2017. Nature and Science, 15(2): pp. 1-13.
- Harben P.W. (1999). The industrial minerals handybook, a guide to markets, specifications and prices (3rd edition). IMIL, Surrey, UK, pp. 270.
- Robert V. (2012). Mineral Commodity Summaries, Technical report, U.S. Geological Survey. pp. 44-45.
- Perry D. L. 2011. Handbook of Inorganic Compounds, Taylor & Francis, 2011, ISBN 978-1-4398-1461-1.
- Krinsley D. H., and Doornkamp J. C. 1973. Atlas of Quartz Sand Surface Textures. Cambridge University Press, Cambridge, pp: 91.
- Madhavaraju J., García Barragán J. C., Hussain S.M., and Mohan S.P. 2009. Microtextures on quartz

- grains in the beach sediments of Puerto Peñasco and Bahia Kino, Gulf of California, Sonora, Mexico, *Rev. Mex. Cienc. Geol.*, 26(2), pp 367-379.
20. Blatt H., Middleton G. V., and Murray R. 1980. *Origin of Sedimentary Rocks*, 2nd ed., Englewood Cliffs, New Jersey: Prentice-Hall.
  21. Morton A. C., Davies J.R., and Waters R.A. 1992. Heavy minerals as a guide to turbidity provenance in the Lower Paleozoic Southern Welsh Basin: a pilot study. *Geol. Mag.*, 129, pp: 573-580.
  22. Zhao H. L., Wang D. X., Cai Y.X., and Zhanga F.C. 2007. Removal of iron from silica sand by surface cleaning using power ultrasound, *Minerals Engineering*, Volume 20, Issue 8, pp. 816-818.